

Article

Development of Clay Tile Coatings for Steep-Sloped Cool Roofs

Anna Laura Pisello *, Franco Cotana, Andrea Nicolini and Lucia Brinchi *

CIRIAF–Interuniversity Research Center on Pollution Control and Environment Protection “Mauro Felli”, University of Perugia, Via Duranti 67, Perugia 06125, Italy; E-Mails: cotana@crbnet.it (F.C.); nicolini.unipg@ciriaf.it (A.N.)

* Authors to whom correspondence should be addressed; E-Mails: pisello@crbnet.it (A.L.P.); brinchi@crbnet.it (L.B.); Tel.: +39-075-585-3914 (L.B.); Fax: +39-075-585-3321 (A.L.P.).

Received: 24 June 2013; in revised form: 15 July 2013 / Accepted: 17 July 2013 /

Published: 24 July 2013

Abstract: Most of the pitched roofs of existing buildings in Europe are covered by non-white roofing products, e.g., clay tiles. Typical, cost effective, cool roof solutions are not applicable to these buildings due to important constraints deriving from: (i) the owners of homes with roofs visible from the ground level; (ii) the regulation about the preservation of the historic architecture and the minimization of the visual environment impact, in particular in historic centers. In this perspective, the present paper deals with the development of high reflective coatings with the purpose to elaborate “cool” tiles with the same visual appearance of traditional tiles for application to historic buildings. Integrated experimental analyses of reflectance, emittance, and superficial temperature were carried out. Deep analysis of the reflectance spectra is undertaken to evaluate the effect of different mineral pigments, binders, and an engobe basecoat. Two tile typologies are investigated: substrate-basecoat-topcoat three-layer tile and substrate-topcoat two-layer tile. The main results show that the developed coatings are able to increase the overall solar reflectance by more than 20% with acceptable visual appearance, suitable for application in historic buildings. Additionally, the effect of a substrate engobe layer allows some further contribution to the increase of the overall reflectance characteristics.

Keywords: cool roofs; pigment characterization; solar spectral optical properties; energy efficiency in buildings; historic buildings; spectrally selective cool colors

1. Introduction

The widespread use of materials with high reflectivity to the solar radiation and high spectral emissivity, *i.e.*, cool materials for building envelope applications, is considered as one of the most effective techniques to reduce energy requirements for cooling [1] and also to mitigate urban heat islands, which are related to higher temperatures registered in urban areas with respect to the rural surroundings [2]. The urban heat island effect [3], in particular, is emphasized by the high density of constructions and paving, together with the lack of green areas, that are responsible for higher absorption of the solar radiation and for the increase of anthropogenic generated heat [4].

The research issue concerning high reflective building envelopes has been investigated through important international research projects [5] which have contributed to encourage the adoption of “cool roof” options for several building typologies, in different climate conditions [6]. Numerical and experimental studies on tens of buildings in the United States and in Europe [7–9] have shown the decrease of the cooling peak load by up to 70% and of the indoor free-floating temperature up to 3 °C in the thermal zones adjacent to the roof, produced by cool roof implementation [10].

Although cool roofs represent acknowledged solutions for energy saving, their application is still limited to high reflective coatings for non-sloped roofs, mainly concerning industrial, commercial, or office buildings [11]. Additionally, these building typologies are characterized by higher internal gains, which tend to increase the energy requirement for cooling and the consequent cool roof efficacy [12]. Nevertheless, especially in European historical cities of the Mediterranean Basin, cool roof applications should also concern many buildings located in historical centers and urban architecture heritage contexts, which are largely responsible for the summer peak of electricity requirement for cooling, and where more invasive retrofit interventions are almost impossible to implement [13]. These contexts are mostly characterized by historic buildings located in very dense urban areas, which roofs are sloped and covered by traditional clay tiles [14], where typical cool roof coatings and membranes are impossible to apply for cultural heritage preservation reasons [15]. Therefore, given the acknowledged role of the envelope and roof performance for building energy saving [16–19], the development of effective solutions specifically focused on possible application in historic European urban contexts has an important role for the optimization of: (i) building thermal-energy performance [20] at inter-building scale [21–23] and (ii) urban comfort and reduction of pollutants’ concentration [24].

2. Motivation and Purpose of the Work

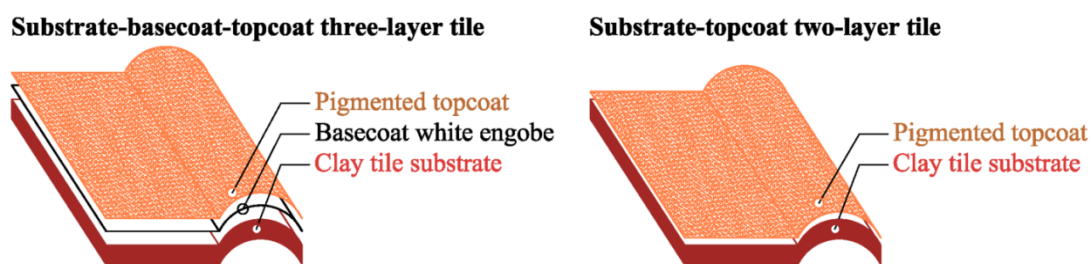
The outlined perspective shows how the investigation of specific coatings for clay represents an important research issue for cool roof development with the purpose to optimize the solar reflectance of traditional buildings’ roofs without affecting their appearance [25]. In particular, this work concerns an investigation of the thermal-optical properties of pigments and binders for clay coatings, which should have equivalent visible characteristics with respect to traditional tiles. In fact, the purpose of this work is the elaboration of high solar reflectance coatings with the same spectral response of traditional clay tiles in the visible region, but high reflectance in other solar spectrum range [26], which includes more than half of the solar radiation [15].

The chosen mineral based coatings are specifically optimized in order to elaborate covering layers for tiles representing non-impacting passive solar techniques which contribute to building energy efficiency and indoor thermal comfort during the cooling season, for possible applications in Italian and European historic buildings [27].

In the choice of materials—tiles, binders, and pigments—traditional and natural building materials and techniques are preferred. In fact, parallel to the concept of cool materials optimization [28], the appreciation of traditional techniques and natural local materials and technical elements, *i.e.*, clay tiles, contributes to the purpose of providing important advantages from a global environment point of view [29–31], such as: low embodied energy, ability to regulate indoor humidity, reduced toxicity, and relatively low price [14].

In order to optimize the final performance of the cool roof, two kinds of tiles are compared: (i) the substrate-topcoat two-layer tile; and (ii) the substrate-basecoat-topcoat three-layer tile (Figure 1). Accordingly, new samples are prepared by applying the same coatings upon two different tile substrates: a natural tile and a novel white-engobe clay tile [14]. Therefore, current investigation is aimed at systematically estimate and optimize the optical and thermal behavior of these two sets of clay tiles, in order to provide a better understanding of factors that play major roles in the performance of cool roof technologies.

Figure 1. The two investigated tile typologies.

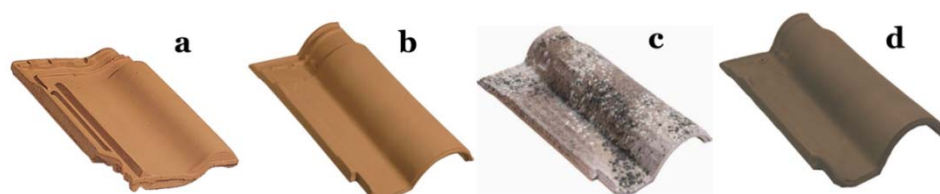


3. Materials and Methods

3.1. Clay Tiles

Clay tiles are the most diffuse roof covering element used in Italian buildings. In particular, clay tiles represent the traditional technique used to direct rain water towards the drainpipes. A typical clay tile is about 42 cm × 25 cm in size, and weighs around 3 kg. The natural colors of the tiles are light brown, red or beige, depending on varying clay pit location (Figure 2a,b), but also different finishes are available in the market in order to reproduce fake ancient effects or other colors (Figure 2c,d).

Figure 2. Typical commercialized clay tiles. (a,b) Natural “terracotta” tiles; (c) Clay tile with old-looking effect; (d) Brown engobe tile.



3.2. Coatings

The chosen pigments and the binder used are easily commercially available at low price. A mineral- based binder with high permeability to aqueous vapor is chosen. The selected white opaque stabilized potassium silicate-based binder addresses DIN 4108.3 and DIN 18363 requirements. It contains TiO_2 pigment: a strongly scattering, weakly absorbing, stable, non-toxic, inexpensive and hence extremely popular white pigment, which also exhibits photocatalytic activity [32]. As regards colored pigments, natural mineral earths are preferred, because of their high stability under weathering conditions, light oxidation and corrosion [33]. Iron oxide-based yellow (encoded with *Y* in Table 1), red (encoded with *R*) and brown (encoded with *B*) are used as pigments.

3.3. Preparation of Samples

Small coupons of 7 cm × 7 cm are cut from tiles and covered with the experimental coatings. The sample name and composition of the coatings are reported in Table 1.

Table 1. Codenames and composition for the elaborated samples.

Sample code	White basecoat	Experimental coating			
		<i>Y</i> (g)	<i>R</i> (g)	<i>B</i> (g)	Opaque binder (g)
N0	no	-	-	-	-
N1	no	-	-	-	100
N1A	no	3.6	-	-	100
N1B	no	7.2	-	-	100
N1C	no	7.2	0.6	-	100
N1D	no	7.2	1.4	-	100
N1E	no	7.2	1.4	1.0	100
N1F	no	7.2	1.4	1.6	100
N1G	no	11.3	1.4	1.6	100
W0	yes	-	-	-	-
W1	yes	-	-	-	100
W1A	yes	3.6	-	-	100
W1B	yes	7.2	-	-	100
W1C	yes	7.2	0.6	-	100
W1D	yes	7.2	1.4	-	100
W1E	yes	7.2	1.4	1.0	100
W1F	yes	7.2	1.4	1.6	100
W1G	yes	11.3	1.4	1.6	100

Colored coatings are prepared in the lab by mixing the opaque white binder with water (as suggested by manufacturer) and with different weighted amounts of pigments, obtaining different colors. The various coatings are prepared in such a way that two consecutive coatings in Table 1 differ in only one added component; using this method of changing one variable at a time, useful comparisons between various coatings are carried out.

The coatings are applied upon the tiles immediately after preparation by means of a paint-brush. The same coating, referred to as “experimental coating” in Table 1, is applied as the only coating in

natural tile (encoded with N in Table 1) and as topcoat over a white engobe basecoat in white tiles (encoded with W in Table 1), as described in Figure 1. The coated tiles are allowed to dry at room temperature for 2 weeks before measurements described in Section 2. The experimental analysis of the samples concerns the evaluation of natural brick tiles and coated tiles, which roughness could be considered as equivalent, in order to evaluate the effect of the pigment in terms of visual appearance (color) and reflectance performance.

4. Experimental Procedure

The analysis of the thermal and optical properties of the clay tile samples is carried out by an integrated experimental analysis consisting of three main phases: (i) the solar reflectance measurement (Figure 3a) and (ii) the thermal emittance measurement (Figure 3b). Additionally, (iii) infrared thermography is used to evaluate the absorbed heat by the tile samples in the same boundary conditions. The used infrared camera is a FLIR B360 (FLIR Systems, Inc., Wilsonville, OR, USA) which characteristics are reported in Table 2.

Figure 3. (a) Spectrophotometer; (b) emissometer instruments for the in-lab experimental analysis.



Table 2. Characteristics of the infrared camera.

Field of view	25°/19°	IR resolution	320 × 240
Minimum focus distance	0.4	Spectral range	7.5 ÷ 13 μm
Thermal sensitivity	0.06 °C	Object temperature range	−20 °C to +120 °C
Detector type	focal plane array	Accuracy	±2% of reading

The spectrophotometer with integrating sphere used in order to characterize the solar reflectance of the samples is a Shimadzu SolidSpec 3700 (Shimadzu Corporation, Kyoto, Japan), which characteristics are reported in Table 3. The solar hemispherical reflectance of the samples is determined by following the procedure described in [34], with reference to the solar spectrum reported in [35].

Table 3. Characteristics of the spectrophotometer.

Spectral bandwidth	UV/VIS: 0.1–8 nm (8 steps) NIR: 0.2–32 nm (10 steps)	IR resolution	320 × 240
Spectrum interval	240 ÷ 2600 nm	Noise	<0.0002 Abs (500 nm, SBW 8 nm), <0.00005 Abs (1500 nm, SBW 8 nm) determined under conditions of RMS value at 0 Abs and 1 s response
Resolution	0.1 nm	Photometric range	−6 to 6 Abs
Wavelength accuracy	UV/VIS: ±0.2 nm, NIR: ±0.8 nm	Accuracy	±2% of reading
Wavelength repeatability	UV/VIS: ±0.08 nm, NIR: ±0.32 nm		

The emittance measurements are carried out AE1 RD1 emissometer with scaling digital voltmeter: the guidelines reported in [36] are followed. The instrument is composed by a differential thermopile radiant energy detector, a heater, a heat sink with a flat surface, two sets of reference standards for the calibration, and the samples to be tested. The samples are prepared in order to be slightly larger (7 cm × 7 cm) than the outer dimensions of the emissometer measuring head, as suggested by [36] international standard. The emittance measurement has a repeatability of ±0.01 emittance units and it approximates total hemispherical emittance at 65 °C. The detector responds to the radiation heat transfer and it produces a voltage output that is linear with emittance.

5. Results and Discussion

5.1. Visual Appearance of the Samples

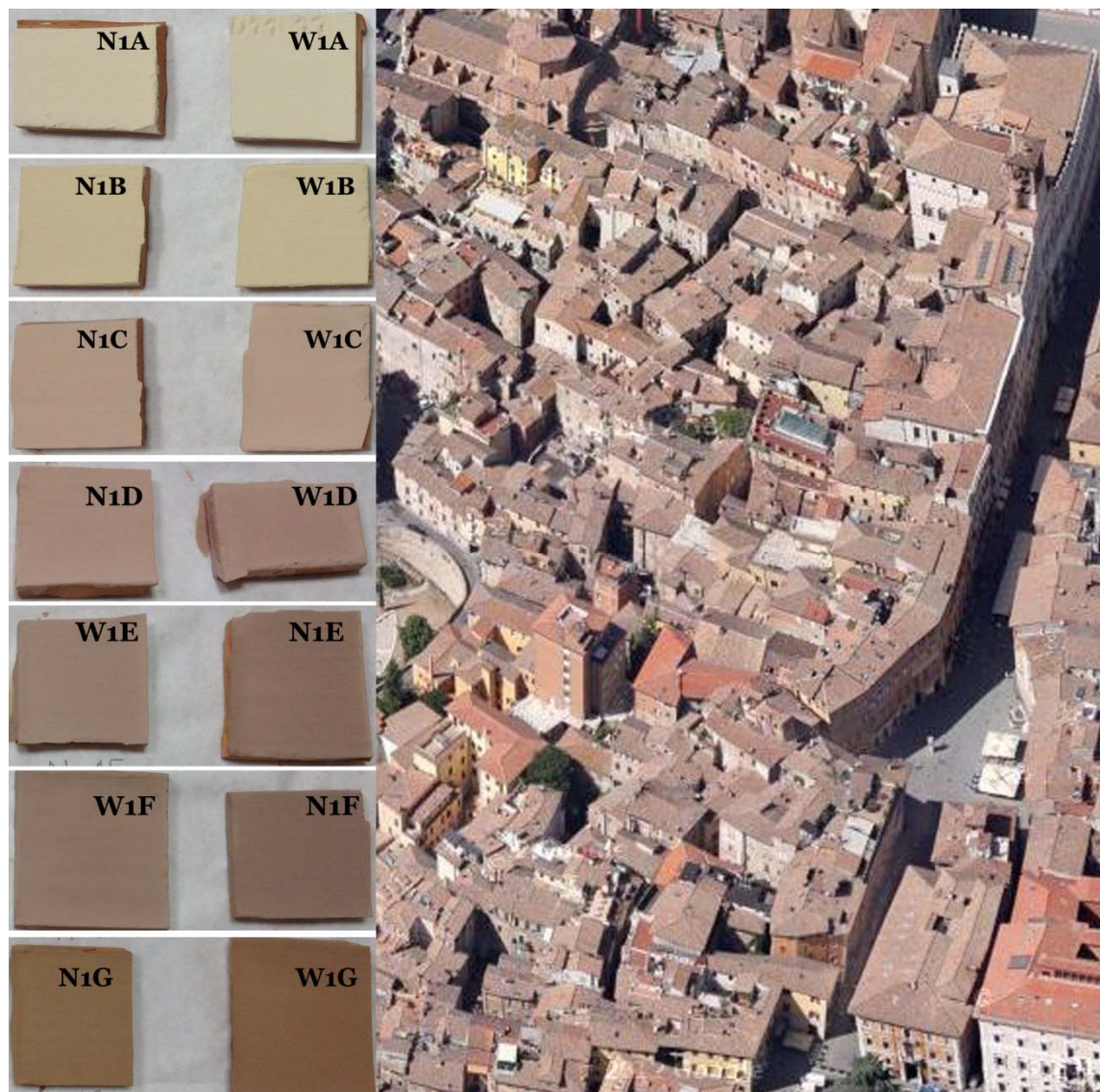
As previously mentioned, the elaboration of the coating consists of a progressive increase of the percentage of colored natural mineral earths into the white opaque mineral based binder. As reported in Figure 4 and in Table 1, the colored pigments are applied step-by-step following this order:

- Yellow pigment: W1A, N1A, W1B, N1B samples;
- Red pigment: W1C, N1C, W1D, N1D samples;
- Brown pigment: W1E, N1E, W1F, N1F, W1G, N1G samples.

Therefore, the darkest samples, *i.e.*, N1G and W1G, present the overall mix of these pigments, which purpose is to obtain a visual appearance of the tile as close as possible to the ancient traditional clay tiles found in Italy (Figure 4). The application of such coatings shows that: (i) the appearance of the tiles is very close to that of natural clay tiles of ancient buildings starting from the C series of samples to the G series, which color is equivalent to the natural clay color; (ii) the final appearance of the tiles does not show any perceivable difference between the natural tile (N series) and the tile with the white engobe (W series) as substrate. This implies that the visible feature of the tiles is mainly attributable to the chosen pigments and to the mineral binder. Therefore, no perceivable effect of the engobe in the visible part of the reflected spectrum is expected, while the purpose is to increase mainly

the infrared reflectance capability of the proposed tiles, where there is about the half of the solar radiation, which represents a key cooling capability to be developed [10].

Figure 4. Elaborated samples and comparison of the visual appearance with respect to the traditional roof tiles of the historic center in Perugia, Italy.



5.2. Infrared Thermography

Infrared thermography was performed on 14 June 2013. This day was chosen for the hot weather conditions, typical of the summer period in most of Italian territory (Figure 5). All the samples were exposed to the solar radiation at about 9:00 a.m. and they were tested under the same weather and exposure conditions all morning long. The overall photography campaign was carried out at the same time (2:00 p.m.) in order to obtain reliable comparative assessment of the superficial temperature of the tiles. Figure 5 represents the daily profile of the main weather parameters impacting the superficial temperature of the samples, and the relative cool roof performance, which have been continuously monitored during that day for the purpose of this study: outdoor dry bulb temperature, wind velocity, global solar radiation of the measurement site. Although the thermography analysis is a preliminary

screening test, it allows us to describe the comparative effect on temperature rise in the sun of the tested samples. The infrared images illustrated in Figure 6 show that the surface of the original natural red tile (N0) is hotter than the other developed clay tile. In particular, the N1 and W1 tiles are colder than the red tile by about 12 °C, while the N1C and W1C tiles, which present less impacting color appearance, present lower (by about 7 °C) superficial temperatures. Finally, N1G and W1G samples are colder with respect to the natural red tile by about 4 °C, despite the equivalent visual appearance. Additionally, the engobe samples seem to be slightly colder than the N-based samples but the precision level of the thermography and the variability of the human measurement position are not reliable enough to outline a definite behavior of the W-samples with respect to the N-samples, which is detailed in Section 4.3.

Figure 5. Main weather parameters continuously monitored during the thermography analysis.

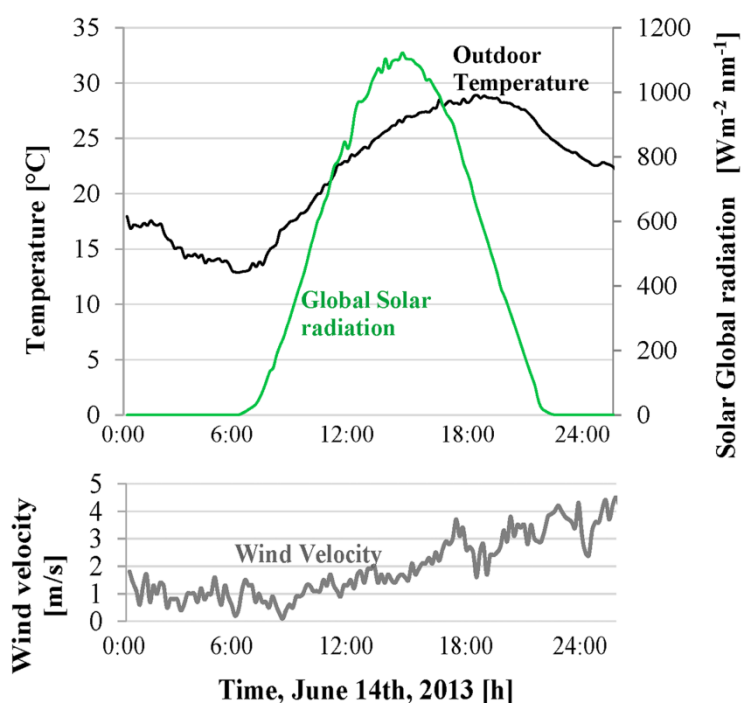
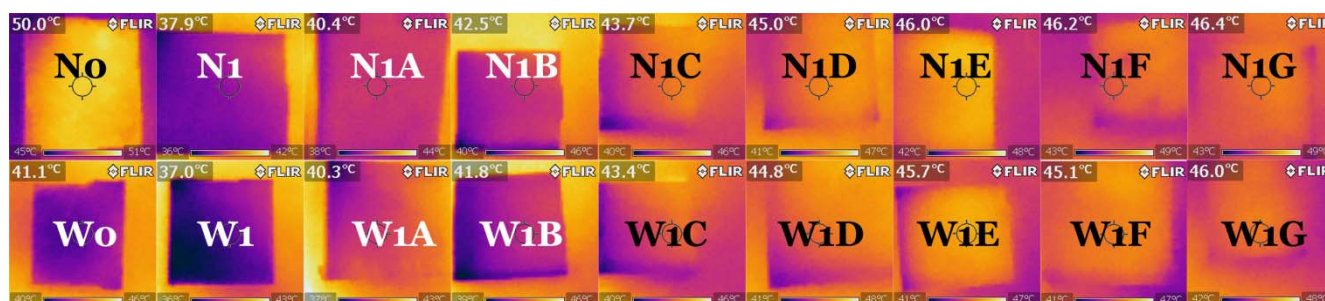


Figure 6. Thermography images of the developed samples.



5.3. Solar Reflectance Spectra

Reflectance spectra of the various samples are reported in Figures 7 and 8. The values of solar reflectance calculated following the procedure detailed in Section 3, by spectrophotometer with integrating sphere, are reported in Table 4. A gradual decrease of reflectance with increasing pigment

content in both sets of tiles is clear from reflectance spectra; such decrease is particularly important in the VIS region, as expected, because the pigments are added to intentionally modify the visual appearance. On the other hand, all 14 of the experimentally colored tile samples exhibit rather good solar reflectance, *i.e.*, $R > 53$, and nine samples have $R > 65$. In order to have a better understanding of the role played by the various components, comparisons are carried out, as shown in Figures 7 and 8.

Figure 7. Solar reflectance of the substrate-basecoat-topcoat 3-layer tiles.

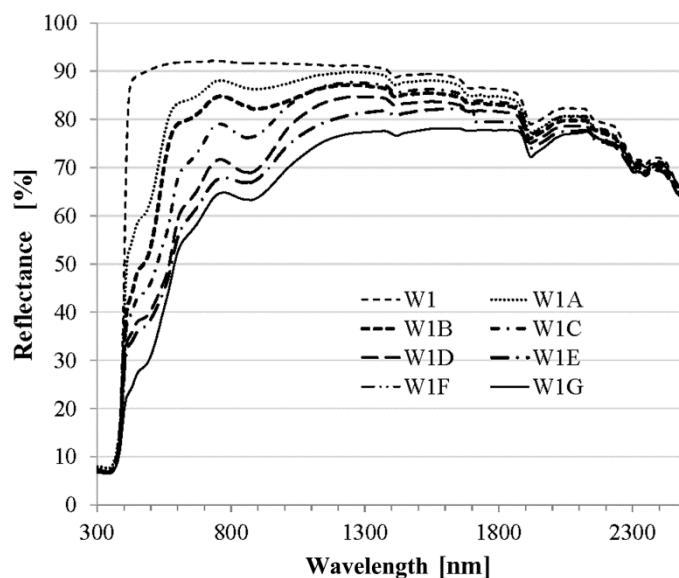


Figure 8. Solar reflectance of the substrate-topcoat 2-layer tiles.

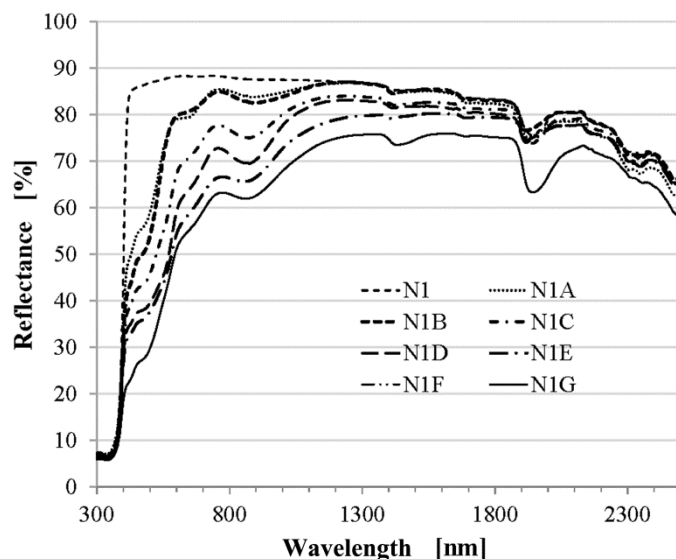


Table 4. Solar reflectance and thermal emittance of the various samples.

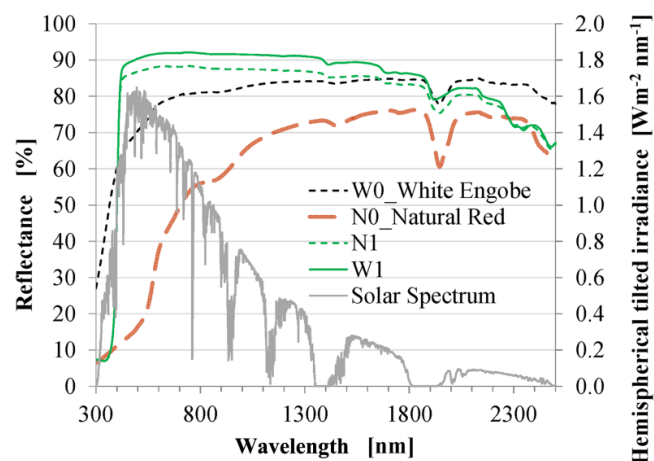
Sample codenames	R_{UV}	$R_{VISIBLE}$	R_{NIR}	$R_{SOLAR} (R)$	IR emittance Emittance (%)
	Reflectance (%)	Reflectance (%)	Reflectance (%)	Reflectance (%)	
	300–380 nm	380.5–780 nm	781–2500 nm	300–2500 nm	
N0	8.8	31.1	65.9	45 ¹	0.88
N1	8.5	85.2	86.2	83	0.89
N1A	8.7	69.7	84.2	74	0.89
N1B	8.0	67.8	83.9	73	0.90
N1C	7.9	58.5	79.6	66	0.89
N1D	7.5	52.1	76.9	61	0.90
N1E	7.7	48.5	73.3	58	0.90
N1F	7.1	45.2	70.3	55	0.90
N1G	6.7	43.4	69.1	53	0.90
W0	45.3	74.1	82.8	77 ²	0.90
W1	8.6	88.6	89.9	87	0.89
W1A	9.1	73.7	86.8	77	0.89
W1B	7.9	67.5	83.8	73	0.89
W1C	8.1	59.1	81.8	67	0.88
W1D	8.2	52.3	77.2	62	0.88
W1E	7.7	48.4	73.1	58	0.88
W1F	7.6	46.8	72.0	56	0.89
W1G	7.3	44.7	71.0	55	0.88

¹ Our value is consistent, although slightly better, than lit. Values of solar reflectance for terracotta ceramic tiles which are in the 25%–40% range [2]; ² This value is consistent, although slightly better, than the lit. Values for white clay tile, which are in the 60%–75% range [2].

5.3.1. Effect of the Binder

Figure 9 reports the solar reflectance of the tile W0 with the white engobe, the natural red terracotta tile N0, and the same two samples (W0 and N0) with the white opaque binder experimental coating, respectively named N1 and W1 (for codenames see Table 1).

Figure 9. Comparison between the solar reflectance of samples to investigate the role of the binder.



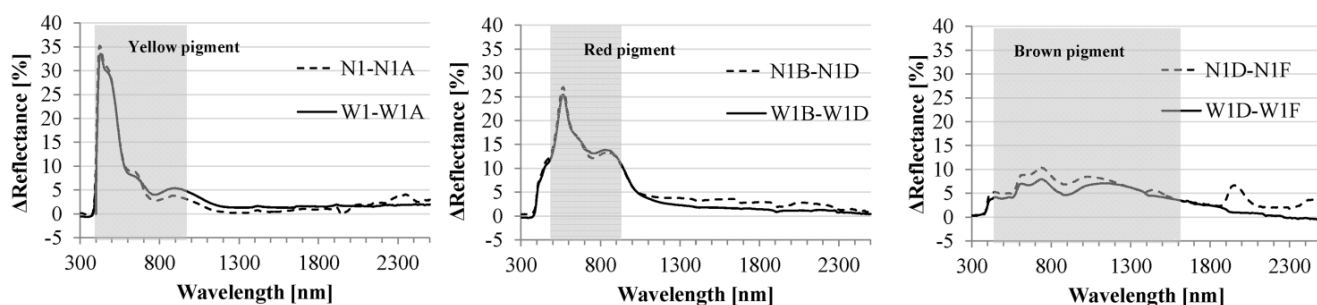
By comparing W0 and N0, it is evident that the engobe is able to produce an important increase of solar reflectance, especially in the most powerful zone of the solar radiation spectrum (grey line), up to 1500 nm, also given the much lighter color of the engobe. In fact, R_{UV} and R_{VIS} values of the W0 sample are higher by 36% and 43%, respectively, with respect to the N0, while in terms of R_{NIR} the difference is 17%. Accordingly, the value of R (Table 4) is much higher for W0 (77%) than for N0 (45%). It is noteworthy that the reflectance of W0 is slightly higher than the values given in the literature for white clay tiles [2].

By comparison of the white coated tiles, N1 and W1, with the engobe tile, W0, Figure 9 clearly shows how the white coating produces a significant increase in reflectance values in the interval 400/1900 nm, and also a brief decrease of reflectance between 300 and 400 nm and beyond 1900 nm. These two contributions to reflectance can be ascribed, respectively, to the content increase of TiO_2 and to absorbance of the binder, including the little amount of organic stabilizers present in it. Therefore, the selected binder has a relatively low impact on the overall solar reflectance capability, with a better performance than organic binders such as acrylic matrix [10]. The overall effect of application of the experimental white coating corresponds to a significant increase in the solar reflectance, R , with values increasing up to 83% and 87% for N1 and W1 respectively, from base values of 45% and 77%, for N0 and W0 respectively (Table 4).

5.3.2. Effect of the Colored Coatings

Selected differential spectra are evaluated [37,38] and reported in Figure 10. In Figure 10a the differences of solar reflectance of experimental coatings 1 and 1A, for both sets of tiles encoded as N and W, are plotted vs. the wavelength. This plot clearly shows the effect of addition of 3.6 g of iron oxide yellow pigment to 100 g of white opaque binder upon the reflectance of the experimental coating. Similarly, in Figure 10b the differences of reflectance vs. the wavelengths of coatings 1B and 1D are reported, showing the effect of addition of 1.4 g of iron oxide red. Additionally, the differences of reflectance between 1D and 1F are reported in Figure 10c, showing the effect of addition of 1.6 g of iron oxide brown pigment.

Figure 10. Evaluation of the effect of colored pigments through differential spectra: (a) Yellow; (b) Red; (c) Brown.



Due to the different amounts used of the various pigments, given the main purpose to reproduce equivalent visual appearance with respect to the traditional “terracotta” tile, and the complexity of the coatings, the comparisons do not pretend to give rigorous insight into the behavior of each pigment. Nevertheless they are aimed at outlining the role played by pigments upon the overall observed

reflectance of the complex systems. It is noteworthy, however, that especially for the simplest of the systems investigated in Figure 10a, the differential spectrum is consistent with the absorption coefficient variation with wavelength of a similar iron-oxide based yellow pigment obtained by a rigorous treatment [25]. In more complex system, *i.e.*, with red and brown pigments, the differences found between the spectra measured in this paper with respect to the literature are more important. Despite that fact, the analyses carried out for the purpose of this work in terms of differential spectra are of some utility, as specified below.

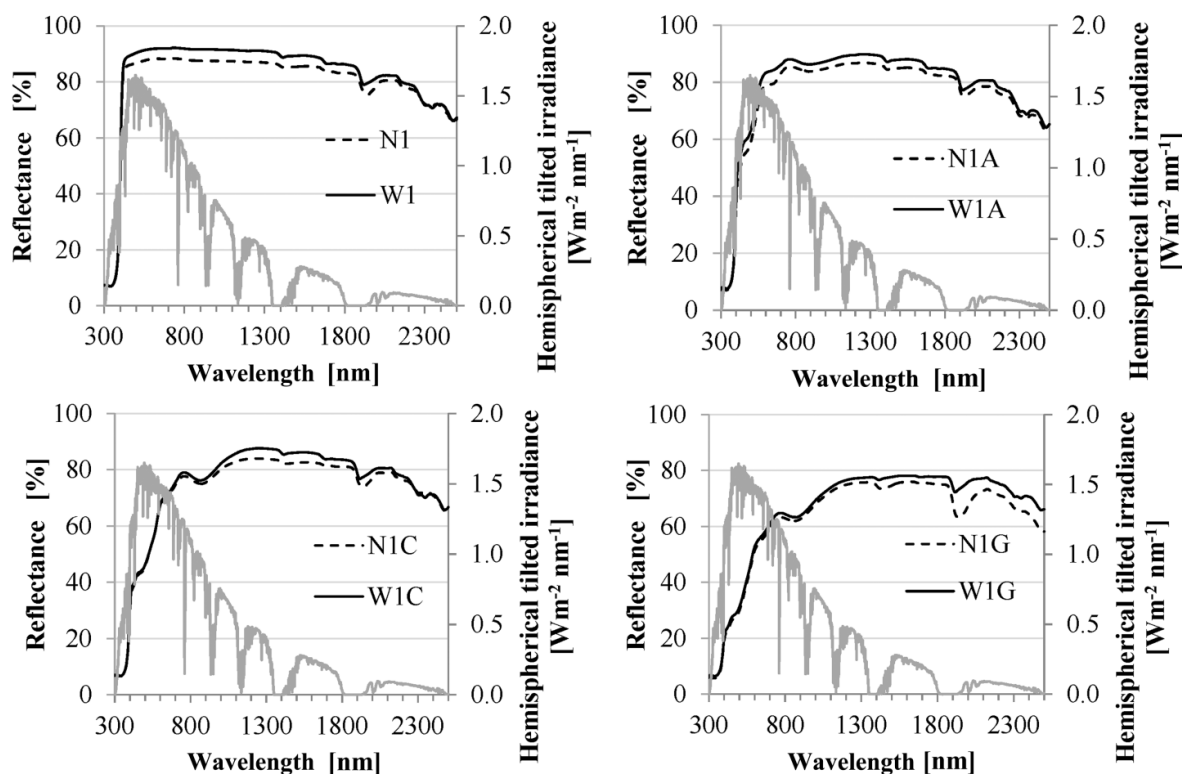
As regards the yellow pigment, Figure 10a shows that spectra are basically similar for the two sets of tiles and that important absorbance is registered in the VIS region around 400–600 nm, while low absorption is registered in the NIR region, with just a small peak around 900 nm. Accordingly, the values of solar reflectance, R , for addition of the yellow pigment (Table 4, samples with codenames 1A and 1B compared with coating 1 for both sets of tiles N and W) decrease by up 17%–18% in the VIS region, but only by about 2% in the NIR region. The overall solar reflectance values are rather good, in the range 73%–77%, which makes this pigment a “cool” coating. However, red and brown addition seems necessary to give the tile a visible appearance similar to the natural terracotta color, as evident from the samples reported in Figure 4. As regards the red, it is clear from Figure 10b that the iron oxide based pigment gives an important contribution to the decreased reflectance observed both in VIS and in NIR regions, especially around 500–1000 nm, whereas its behavior is cooler at wavelengths above 1000 nm. Its addition leads to a decrease in the values of reflectance by up to 22% in VIS and 7% in NIR, but the overall values of R are still good, in the range 61%–67% (Table 4). As regards the brown, the differential spectra in Figure 10c give an indication of a relatively small contribution of this pigment in the VIS region (if compared to yellow and red pigments), and this can be rationalized as related to a leveling effect. Anyhow, brown pigment contributes to decrease of reflectance in the wavelength range up to 1600 nm, and R decreases to values in the range 53%–56% (Table 4). These values can be considered as a good result for a relatively dark colored tile, in particular if compared to the natural red tile, which solar reflectance corresponds to 45%, with the same visible appearance of N1G and W1G (Figure 4).

5.3.3. Effect of the White Engobe Basecoat

The effect of the basecoat, *i.e.*, engobe layer, is now assessed in order to analyze its possible role in emphasizing the solar reflectance when topcoat colored pigments are applied. Figure 11 reports reflectance spectra of both kinds of tiles (N and W) with some of the opaque experimental coatings used, for a rapid visualization of the effect of the engobe. The solar spectrum is also reported in order to gain immediately the idea of the relative importance of the spectral region in terms of solar irradiance. It is clear that the engobe produces a beneficial effect on the overall performance of all the tiles investigated. The major effect is observed in white tiles, with higher values of reflectance in the region 400–1900 nm (Figure 11), and higher values of R by about 4% points (Table 4) for W1 with respect to N1. On addition of the pigments, the beneficial effect of the engobe is less important, but it is still present although it does not give any effect in terms of visual appearance. In fact, in presence of the engobe basecoat, reflectance is higher in the region 400–2300 nm for yellow (Figure 11, N1A, W1A), and in 900–2200 nm for red (Figure 11, N1C, W1C), and in 900–2500 nm for brown (Figure 11,

N1G, W1G). For colored tiles the values of R are generally higher in presence of the engobe basecoat by 1%–4% points (Table 4).

Figure 11. Solar reflectance comparison between samples with and without the basecoat engobe.



6. Concluding Remarks and Perspectives

The current work examined the behavior of new tiles developed in order to evaluate possible innovative cool roof applications specifically fitting with the traditional Italian and European context, in particular for possible application to historic buildings, which energy efficiency retrofits are much restricted by specific constraints due to the preservation of the architectural heritage. In fact Italian regulation imposes heavy limits about the implementation of systems and technologies impacting ancient buildings and environmentally protected areas. These limits represent the boundary conditions of this research and the objective of the experimental study at the same time. The development of these innovative tiles is effectively aimed at elaborating high performance tiles in terms of cool roof potential, but with the same visual appearance of traditional “terracotta” tiles.

To this aim, new tile prototypes were prepared, consisting of traditional clay tiles where colored opaque coatings were applied with a visual appearance essentially the same of the existing traditional “terracotta” tiles. Two kinds of tiles are compared: (i) the substrate-topcoat two-layer tile; and (ii) the substrate-basecoat-topcoat three-layer tile. Accordingly, new samples were prepared by applying the same coatings upon two different tile substrates, a natural tile and a novel white-engobe clay tile. The experimental methodology consisted of: a screening test by thermography, a spectrophotometer and emittance analysis, a final deep analysis of the solar reflectance spectra profile for different wavelength bands. In the same monitored weather conditions, the thermography allowed to find out different

superficial thermal behavior of the samples, which presented colder surface temperature with increasing visual clarity of the appearance. Moreover, even the darkest prototyped tile presents lower superficial temperature by about 4 °C than natural red tile. The spectrophotometer analysis allowed to characterize the solar reflectance spectra of the samples and to identify the influence of: (i) the binder; (ii) the several colored pigments; (iii) the engobe basecoat layer.

First results showed that, if a white tile can be used, tile W0 with $R = 77\%$ is an optimal choice for a new roof, with a good ratio performance/cost because the engobe can be directly applied at the factory, following the same procedure of industrially colored tiles, at low cost. Additionally, the durability performance of the engobe has the same guarantee of the tile element itself, which represents an important benefit in terms of the maintenance of the cool roof effect for decades. If a layer of the experimental coating is added, the value of the global solar reflectance, R , goes up to 87%, with the relative benefits in terms of the overall performance of the cool roof system. On the other hand, for existing roofs, application of the experimental coating 1 over traditional tiles is an effective and simple option, with high performance ($R = 83\%$) and a rather significant improvement with respect to natural terracotta tiles, although the labor cost should be included into the overall evaluation.

Finally, in historical centers where white tiles cannot be used, a weakly light red coating with relatively high increase of solar reflectance, is represented by the 1C coating, with $R = 66\%$ – 67% . If the dominant color of the area is even darker, a still effective coating for tile is 1F or the darker 1G, with $R = 53\%$ – 56% . These two colored coatings would lead to an important improvement in cooling while maintaining basically the same visual aspect of traditional “terracotta” tiles. In fact, the values of solar reflectance, R , are increased with respect to natural tile N0 by a factor of up 50% for 1C, and up to 22% for the darkest tile 1G. Additionally, in the case of colored tiles, the presence of the white engobe basecoat gives an overall improvement of 1–4 percentage points in terms of solar reflectance. Therefore, specific case study analyses should investigate the cost-effectiveness of this solution with different boundary conditions. In this work, the preliminary assessment of the cost-effectiveness of the proposed tiles is carried out by considering several published results [11] where the effect of increased reflectance is evaluated in different climates, when cool roofs are applied to residential buildings. In particular, the estimated effect in Italian climate corresponds to about 25% and 17% of reduction of discomfort hours in summer, in Palermo and Rome, Italy, respectively. [11]. The primary energy saving for cooling is 33% and 30% in Palermo and Rome, when a cool roof with the characteristics of the proposed 1C coating is applied, corresponding to an increase of solar reflectance by about 40% with respect to the base case. It was also demonstrated that the corresponding winter penalty is much less important than the cooling benefit for Mediterranean climates. Additionally, these year-round benefits are even higher for low or non-insulated constructions, which represent the majority of Italian historic buildings.

For all the new tiles presented in this current work, experiments about weathering are in due course. The effect of the tile roughness will be also evaluated, and the weathering performance of the proposed tiles will be compared with existing rougher tiles. On the other hand, other tiles are currently under preparation, with the aim to further increase the performance, with increased amount of the TiO_2 white pigment in the basecoat.

Future developments of this research will deal with the analysis of new pigments, through mixing metals' oxides, and new binders, developed in-lab, where also the dimension of the particles will be

investigated, in order to develop innovative nano-based cool coatings. Finally, the application to a real case study building will be examined, with the final purpose to investigate both the thermal-energy and the economic implications of such an application in Italian historic buildings.

Acknowledgments

Authors' acknowledgments are due to Gloria Pignatta for having contributed to the in-lab measurements, and to Leandro Lunghi who prepared the clay tile substrate samples.

Conflict of Interest

The authors declare no conflict of interest.

References

1. Synnefa, A.; Saliari, M.; Santamouris, M. Experimental and numerical assessment of the impact of increased roof reflectance on a school building in Athens. *Energy Build.* **2012**, *55*, 7–15.
2. Santamouris, M.; Synnefa, A.; Karlessi, T. Using advanced cool materials in the urban built environment to mitigate heat islands and improve thermal comfort conditions. *Sol. Energy* **2011**, *85*, 3085–3102.
3. Akbari, H.; Konopacki, S. Energy effects of heat-island reduction strategies in Toronto, Canada. *Energy* **2004**, *29*, 191–210.
4. Oke, T.R.; Johnson, D.G.; Steyn, D.G.; Watson, I.D. Simulation of surface urban heat island under “ideal” conditions at night—Part 2: Diagnosis and causation. *Bound. Layer Meteorol.* **1991**, *56*, 339–358.
5. Synnefa, A.; Santamouris, M. Advances on technical, policy and market aspects of cool roof technology in Europe: The Cool Roofs project. *Energy Build.* **2012**, *55*, 35–41.
6. Synnefa, A.; Santamouris, M.; Apostolakis, K. On the development, optical properties and thermal performance of cool colored coatings for the urban environment. *Sol. Energy* **2007**, *81*, 488–497.
7. Bozonnet, E.; Doya, M.; Allard, F. Cool roofs impact on building thermal response: A French case study. *Energy Build.* **2011**, *43*, 3006–3012.
8. Zinzi, M.; Agnoli, S. Cool and green roofs. An energy and comfort comparison between passive cooling and mitigation urban heat island techniques for residential buildings in the Mediterranean region. *Energy Build.* **2012**, *55*, 66–76.
9. Pisello, A.L.; Cotana, F. The thermal effect of an innovative cool roof on residential buildings in Italy: Results from two years of continuous monitoring. *Energy Build.* **2013**, submitted for publication.
10. Libbra, A.; Tarozzi, L.; Muscio, A.; Corticelli, M.A. Spectral response data for development of cool coloured tile coverings. *Opt. Laser Technol.* **2011**, *43*, 394–400.
11. Synnefa, A.; Santamouris, M.; Akbari, H. Estimating the effect of using cool coatings on energy loads and thermal comfort in residential buildings in various climatic conditions. *Energy Build.* **2007**, *39*, 1167–1174.

12. Santamouris, M.; Papanikolaou, N.; Livada, I.; Koronakis, I.; Georgakis, C.; Argiriou, A.; Assimakopoulos, D.N. On the impact of urban climate to the energy consumption of buildings. *Sol. Energy* **2001**, *70*, 201–216.
13. Pisello, A.L.; Bobker, M.; Cotana, F. A building energy efficiency optimization method by evaluating the effective thermal zones occupancy. *Energies* **2012**, *5*, 5257–5278.
14. Pisello, A.L.; Rossi, F.; Cotana, F. On the Impact of Cool Roofs in Italian Residential Buildings: Experimental Assessment of Summer and Winter Performance. In Proceedings of SEBUA-12 ICHMT International Symposium on Sustainable Energy in Buildings and Urban Areas, Kusadasi, Turkey, 14–20 July 2012.
15. Libbra, A.; Muscio, A.; Siligardi, C.; Tartarini, P. Assessment and improvement of the performance of antisolateral surfaces and coatings. *Prog. Org. Coat.* **2012**, *72*, 73–80.
16. Asdrubali, F.; Cotana, F.; Messineo, A. On the evaluation of solar greenhouse efficiency in building simulation during the heating period. *Energies* **2012**, *5*, 1864–1880.
17. Buratti, C.; Moretti, E. Lighting and energetic characteristics of transparent insulating materials: Experimental data and calculation. *Indoor Built. Environ.* **2011**, *20*, 400–411.
18. Lai, C.M.; Wang, Y.H. Energy-saving potential of building envelope designs in residential houses in Taiwan. *Energies* **2011**, *4*, 2061–2076.
19. Berardi, U.; Albino, V. Green buildings and organizational changes in Italian case studies. *Bus. Strategy Environ.* **2012**, *21*, 387–400.
20. Pisello, A.L.; Goretti, M.; Cotana, F. A method for assessing buildings' energy efficiency by dynamic simulation and experimental activity. *Appl. Energy* **2012**, *97*, 419–429.
21. Pisello, A.L.; Taylor, J.E.; Xu, X.; Cotana, F. Inter-building effect: Simulating the impact of a network of buildings on the accuracy of building energy performance predictions. *Build. Environ.* **2012**, *58*, 37–45.
22. Xu, X.; Taylor, J.E.; Pisello, A.L.; Culligan, P. The impact of place-based affiliation networks on energy conservation: An holistic model that integrates the influence of buildings, residents and the neighborhood context. *Energy Build.* **2012**, *55*, 637–646.
23. Xu, X.; Pisello, A.L.; Taylor, J.E. Simulating the Impact of Building Occupant Peer Networks on Inter-Building Energy Consumption. In Proceedings of the 2011 Winter Simulation Conference, Phoenix, AZ, USA, 11–14 December 2011; doi:10.1109/WSC.2011.6148033, pp. 3373–3382.
24. Santamouris, M. Heat island research in Europe—The state of the art. *J. Adv. Build. Energy Res.* **2007**, *1*, 123–150.
25. Levinson, R.; Berdahl, P.; Akbari, H. Solar spectral optical properties of pigments—Part II: Survey of common colorants. *Sol. Energy Mater. Sol. Cells* **2005**, *89*, 351–389.
26. Ferrari, C.; Libbra, A.; Muscio, A.; Siligardi, C. Energy performance of opaque building elements in summer: Analysis of a simplified calculation method in force in Italy. *Energy Build.* **2013**, *64*, 384–394.
27. Levinson, R.; Akbari, H.; Reilly, J.C. Cooler tile-roofed buildings with near-infrared-reflective non-white coatings. *Build. Environ.* **2007**, *42*, 2591–2605.
28. Kolokotsa, D.; Maravelaki-Kalaitzaki, P.; Papantoniou, S.; Vangeloglou, E.; Saliari, M.; Karlessi, T.; Santamouris, M. Development and analysis of mineral based coatings for buildings and urban structures. *Sol. Energy* **2012**, *86*, 1648–1659.

29. Dall'O', G.; Speccher, A.; Bruni, E. The green energy audit, a new procedure for the sustainable auditing of existing buildings integrated with the Leed protocols. *Sustain. Cities Soc.* **2012**, *3*, 54–65.
30. Cotana, F.; Rossi, F.; Nicolini, A. Evaluation and optimization of an innovative low-cost photovoltaic solar concentrator. *Int. J. Photoenergy* **2011**, *2011*, doi:10.1155/2011/843209.
31. Rossi, F.; Nicolini, A. Ethanol reforming for supplying molten carbonate fuel cells. *Int. J. Low-Carbon Technol.* **2013**, *8*, 140–145.
32. Bettoni, M.; Brinchi, L.; Del Giacco, T.; Germani, R.; Meniconi, S.; Rol, C.; Sebastiani, G.V. Surfactant effect on titanium dioxide photosensitized oxidation of 4-dodecyloxybenzyl alcohol. *J. Photochem. Photobiol. A* **2012**, *229*, 53–59.
33. Bikiaris, D.; Daniilia, S.; Sotiropoulou, S.; Katsimbiri, O.; Pavlidou, E.; Moutsatsou, A.P.; Chrysoulakis, Y. Ochre-differentiation through micro-Raman and micro-FTIR spectroscopis: Application on wall paintings at Meteora and Mount Athos, Greece. *Spectrochim. Acta A* **2000**, *56*, 3–18.
34. *Standard Test Method for Solar Absorptance, Reflectance, and Transmittance of Materials Using Integrating Spheres*; ASTM E903-96; American Society for Testing and Materials: West Conshohocken, PA, USA, 1996.
35. *Standard Tables for Reference Solar Spectral Irradiances: Direct Normal and Hemispherical on 37° Tilted Surface*; ASTM G173-03; American Society for Testing and Materials: West Conshohocken, PA, USA, 2012.
36. *Standard Test Method for Determination of Emittance of Materials Near Room Temperature Using Portable Emissometers*; ASTM C1371-04a; American Society for Testing and Materials: West Conshohocken, PA, USA, 2010.
37. Brinchi, L.; Germani, R.; Savelli, G.; di Michele, A.; Onori, G. Premicelles of cetyltrimethylammonium methanesulfonate: Spectroscopic and kinetic evidence. *Coll. Surf. A* **2009**, *336*, 75–78.
38. Di Michele, A.; Germani, R.; Pastori, G.; Spreti, N.; Brinchi, L. Effects of temperature on micellar-assisted bimolecular reaction of methylnaphthalene-2-sulphonate with bromide and chloride ions. *J. Colloid Interface Sci.* **2013**, *402*, 165–172.